USE OF MOBILE MEASUREMENTS TO INVESTIGATE FRONTAL STRUCTURES IN MISSISSIPPI

Loren White

Jackson State University, Jackson, MS 39217

Corresponding Author: Loren White, E-mail: Loren.D.White@jsums.edu

ABSTRACT

Two cases of differently oriented frontal systems within Mississippi are investigated using data from a mobile vehicle-mounted observing system in addition to standard atmospheric data sources. Results highlight the capability of the mobile system to diagnose thermodynamic features at a wide range of spatial scales. Widely recognized frontal characteristics are noted in the data, together with some variations. Variations include a lack of strong relationship between frontal position and rainfall bands when examined at small scales. In one case a seemingly anomalous narrow band of significantly lower humidity was identified within about 20 km of the front. These results are indicative of the need for multi-scale data sources and for careful consideration of departures from classical models of phenomena for specific cases.

Keywords: Cold front, temperature, humidity, Mississippi, spatial scales

INTRODUCTION

Since the earliest of the polar front concept by Bjerknes and Solberg (1922) and the later examination by Sanders (1955) and Shapiro (1984), the detailed structure of atmospheric frontal boundaries has been investigated by various means. In recent decades the capability to measure various parameters by aircraft (Blumen et al. 1996) and remote sensing systems (Bluestein et al. 2017; Demoz et al. 2005; Friedrich et al. 2008a; Geerts et al. 2006; Mahre et al. 2017; Wakimoto and Bosart 2000) has led to advances in understanding processes in and near frontal zones. While each measurement methodology has its specific value in describing some aspect of the atmospheric conditions, little attention has yet been given to the use of mobile (i.e. moving) surface-based observing systems to document horizontal variations across frontal zones (White 2014). This is in contrast to much more widespread use of "mobile mesonets" in studies of drylines and severe storms (e.g. Pietrycha and Rasmussen 2004).

Although atmospheric fronts are most rigorously understood in a three-dimensional physical context and may extend throughout the depth of the troposphere, their character and processes near the earth's surface are particularly affected by the nature and condition of the surface. In many respects, fronts observed over flat terrain with uniform low vegetation (e.g. U.S. Great Plains) or over oceanic areas may be considered to be ideal simple cases. Frontal interactions with surface processes in rugged terrain or areas of heterogeneous land use mosaics (forest, urban, crops, small water bodies) are naturally more complex and specific to local geography. Although Mississippi does not have true mountains, the physical geography and biosphere interactions are sufficient to impact fronts in various ways.

It has also become clear from studies over the last few decades that even in simple landscapes the classical conceptual models of fronts do not accurately portray the range of structures observed in all fronts or at all stages of their development and weakening (Koch and Clark 1999, Doswell and Haugland 2007). It is

within this growing awareness of the wide variety of fronts when viewed in detail that the use of measurements from a mobile observing platform, the Jackson State University Mobile Meteorology Unit (MMU), has been developed to facilitate case studies of fronts in Mississippi.

DATA SOURCES AND METHODS

instrumentation used for the Jackson State University MMU were identical to what was reported in White (2014). A Campbell Scientific HMP45C temperature and relative humidity sensor was mounted above the cabin of a standard passenger vehicle within a 41003 Gill radiation shield to minimize direct of the sensor by solar radiation. Geographic position was determined by a Garmin GPS16-HVS system. Data were logged at 10-s intervals onto a CR23X datalogger. In post-processing, dewpoint was calculated from temperature and relative humidity. Using altimeter setting interpolated from surrounding synoptic observing stations, other derived quantities such as potential temperature and water mixing ratio were determined. The advantage of potential temperature is to adjust temperatures to a standard pressure (1000 hPa) so that it is conserved for adiabatic vertical motions and directly proportional to internal energy. Similarly mixing ratio is a direct measure of the amount of water vapor in g/kg.

For comprehensive analysis, surface observations from various synoptic and mesonet observing systems have been utilized (White and Finney 2005). These include METAR-encoded ASOS/ AWOS, RAWS, SCAN, and the weather stations operated by Jackson State University. National Weather Service NEXRAD radar data were obtained in georeferenced format from the Iowa Environmental Mesonet website (https://mesonet.agron.iastate.edu/) and radiosonde data were retrieved NOAA ESRL site (https://ruc.noaa.gov/raobs/). Environmental Mesonet website (https:// mesonet. agron.iastate.edu/) and radiosonde data were retrieved from the NOAA ESRL site (https://ruc.noaa.gov/raobs/).

DECEMBER 2012 COLD FRONT

Early on the morning of 10 December 2012 a strong cold front extended from a large low-pressure system over the Great Lakes through the Mississippi Delta down to South Texas (Fig. 1). The MMU made a transect between Jackson and Indianola, Mississippi from 0823 to 1205 UTC (2:23-6:05 AM Central Standard Time) to intercept this front. The local synoptic conditions are summarized in Fig. 2.a. The warm air mass southeast of the cold front was typified by temperatures ranging from 16 to 22 C, southerly flow from the Gulf of Mexico, and dewpoints from 11 to 15 C. At the front the wind suddenly shifted to northwesterly and temperatures began to drop, initially by a few degrees but continuing to well below freezing (-5 C) in the Ozarks. The northbound MMU intercept of the front was at 0953 UTC about 15 km south of Indianola. On the return trip it was intercepted about 15 km north of Yazoo City at 1058 UTC, indicating that the front moved at an average of 35 km/hr during the period. Most analysis and discussion will be focused on the northbound transect. In order to focus more directly on conservative quantities, the analysis will be primarily in terms of potential temperature and mixing ratio instead of temperature and dewpoint. The MMU of temperature measurements in context surrounding station data are summarized in Fig. 2.b.

As demonstrated by the radar reflectivity (Fig. 2.c), most of the transect was in moderate rain. It is of interest that there was no obvious relationship of precipitation and the between the intensity exact location of the front. Since the Gill shield was primarily designed to shelter the temperature/ humidity sensor from solar radiation instead of windblown rain, mobile measurements while significant rain must be evaluated for the impact of "wetbulbing" (Straka et al. 1996). The concept is that if the sensor itself becomes wetted by blowing rain then it will end up measuring a temperature that approximately corresponds to the wetbulb temperature of an evaporating saturated surface. This is particularly problematic if the actual relative humidity is significantly below 100%, so evaporative cooling is more effective. To check against wetbulbing, the MMU temperatures relative humidity were compared against nearby

observing stations (KHKS, Mayday, Silver City, and Beasley Lake). Since the effect tends to be cumulative, it would be expected to worsen over time during the nearly continuous rain. Therefore quantitative analysis of the southbound transect is more questionable and the largest impact on the northbound transect should be near Beasley Lake (the northernmost station). The expectation is that wetbulbing should cause

the mobile temperatures to be too low and high. comparison humidity too However between Beasley Lake and the closest mobile observation to it indicate that the MMU temperature was 0.25 C higher (well within the expected variation from siting and sensor differences). So it seems that nearly saturated conditions prevented any significant evaporative cooling regardless of whether the sensor was wetted. Comparisons at the other stations were similar.

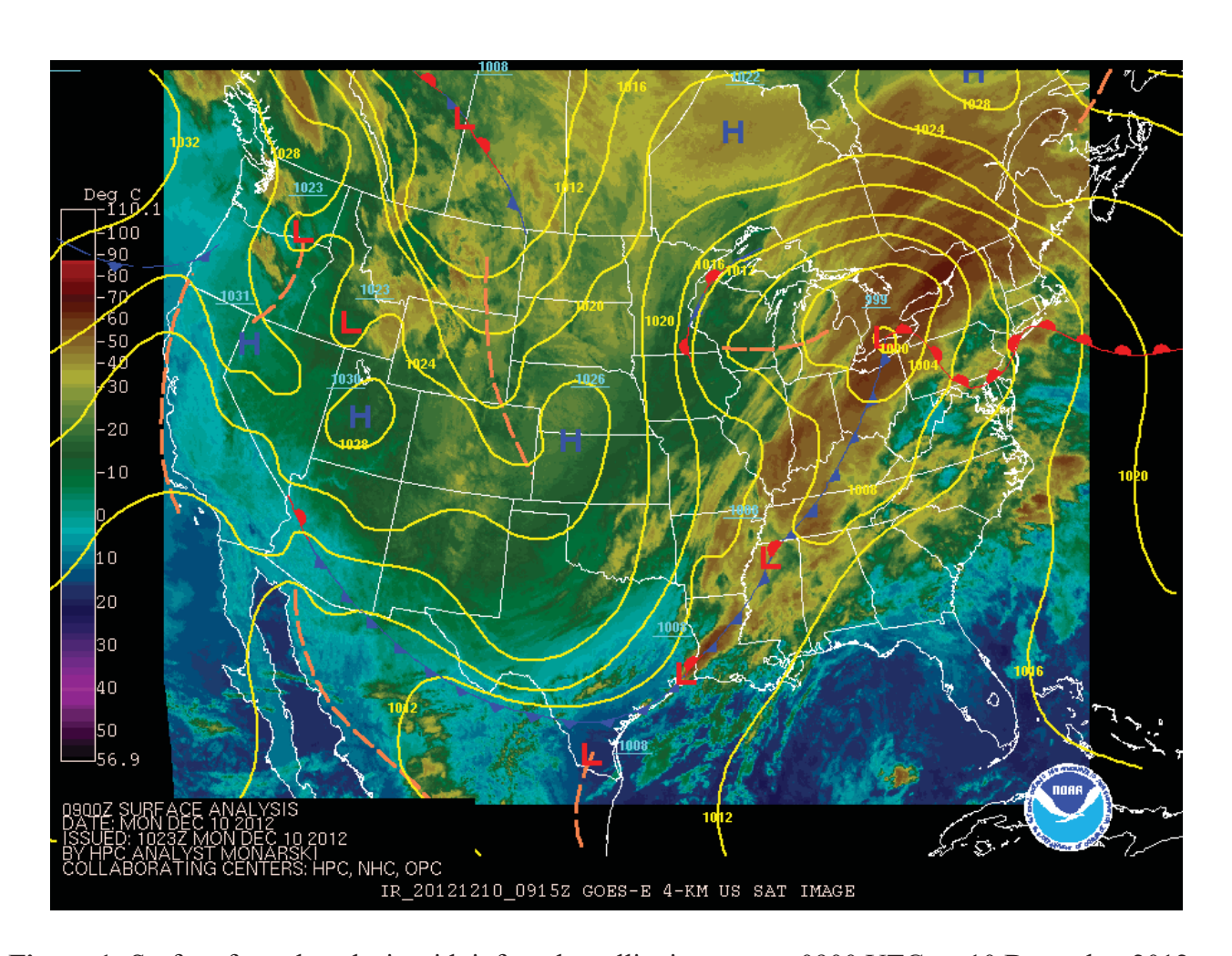


Figure 1: Surface frontal analysis with infrared satellite imagery at 0900 UTC on 10 December 2012.

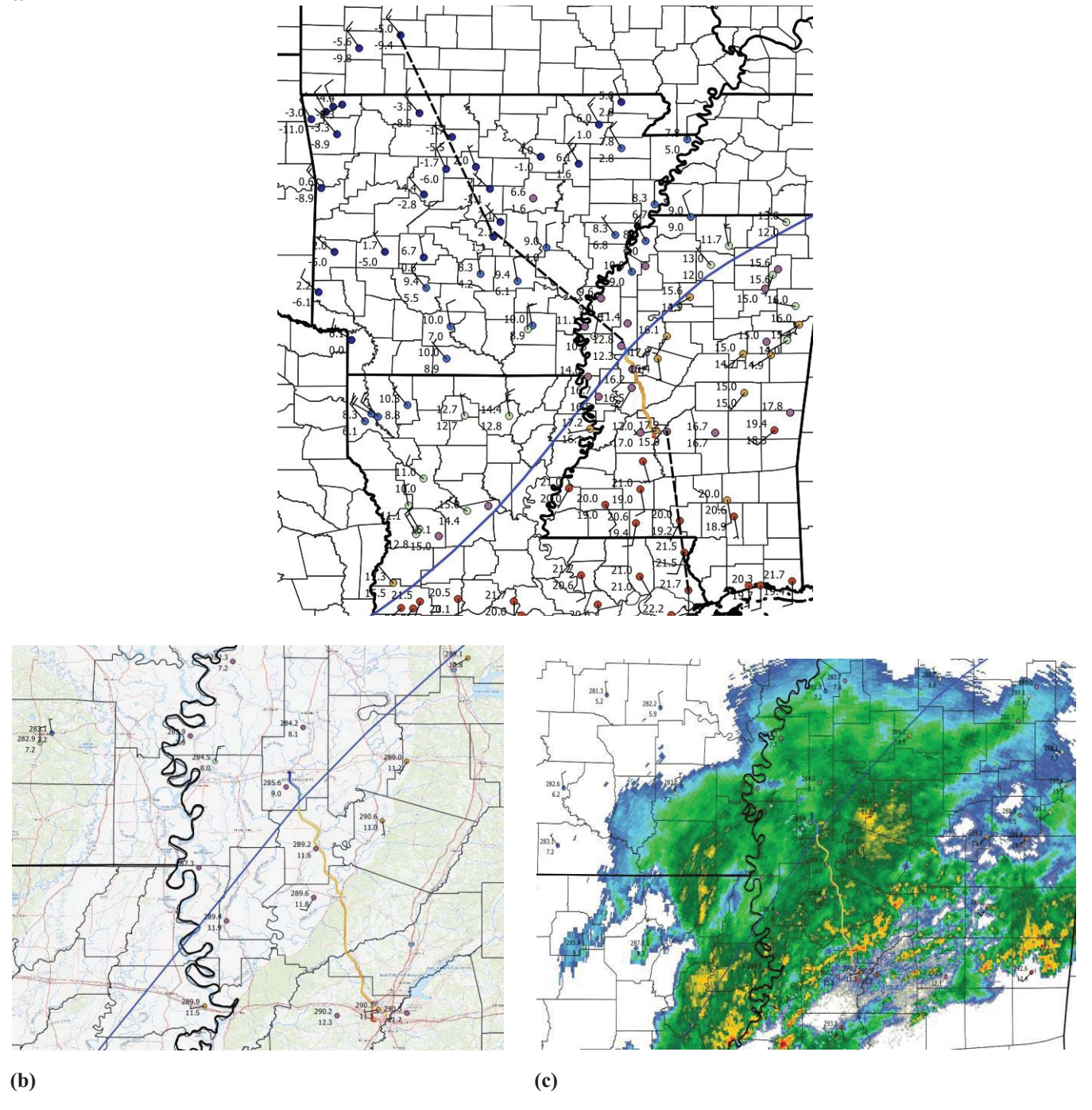


Figure 2: Surface weather conditions and cold front analysis from fixed stations and mobile platform, adjusted to time of northbound front intercept (0953 UTC). Thick blue line indicates cold front. **a)** Regional view, with location of cross-section shown by black dashed line. Station temperature in upper left (C); dewpoint in bottom left (C); winds in kt. Temperature from mobile platform indicated by color (red = maximum; blue = minimum). **b)** Local view near mobile transect. Station potential temperature in upper left (K); mixing ratio in bottom left (g/kg); winds in kt. Potential temperature from mobile platform indicated by color (red = maximum; blue = minimum). Note that most SCAN stations in the Mississippi Delta do not measure winds. **c)** Local view with overlay of radar reflectivity from KDGX (Brandon, MS).

Although the time span of the northbound transect was only 1.5 hr, the rapid cooling behind the cold front and effect of the frontal motion itself compound to complicate determination of conditions at a single standard time. Using a of temperature comparisons combination between north and southbound measurement together with station observations, spatially variable temperature tendencies are applied to adjust the northbound data to a standard time at the front intercept of 0953 UTC. The greatest hourly temperature tendency following the front at nearby stations was -4.3 C/hr at Mayday and the greatest from the north/south mobile data was

-6.8 C/hr. The raw and adjusted potential temperature are shown in Fig. 3. Ahead of the cold front, the potential temperature is quite uniform between 290-291 K north of 32.4 N. South of 32.4 N (in the Jackson Metro area) a mesoscale thermal boundary was associated with the leading edge of the rain-cooled air. The very sudden drop of potential temperature at approximately 33.3 N corresponds to the position of the cold front. The strongest thermal gradient occurs within the first few km and then varies somewhat on the remainder of the track to Indianola.

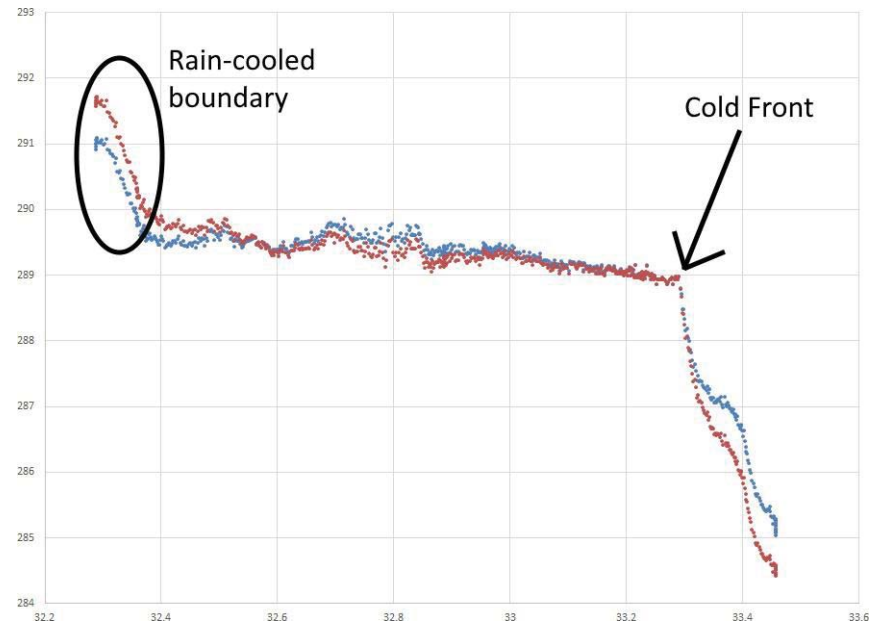


Figure 3: Potential temperature from northbound transect: blue = adjusted for tendencies; red = raw. Valid time 0953 UTC, corresponding to northbound front intercept.

To examine the three-dimensional structure of the front, vertical profiles from the 0900 and 1200 UTC initial model conditions of the operational North American Mesoscale (NAM) model were obtained from the READY archive of the NOAA Air Resources Lab (https://www.ready.noaa.gov; Rolph et al. 2017). The grid spacing of the model at the time was 32 km. Profile locations were chosen at nine points extending between the Slidell, Louisiana

and Springfield, Missouri radiosonde sites, connecting intermediate radiosonde sites and the endpoints of the mobile transect. To verify that the model adequately matched with observed conditions, the vertical profiles were compared against 1200 UTC radiosonde data (e.g. Fig. 4.a).

For synthesis with the observed surface data, NAM profiles were interpolated to 1000 UTC. Using the combination of NAM profiles, nearby surface observing sites, and MMU data adjusted to 0953 UTC, a cross-section analysis of potential temperature was constructed (Fig. 4b). The pattern matches well with similar frontal analyses (Sanders 1955, Miller et al. 1996,



Friedrich et al. 2008), showing a relatively well-mixed layer below 1 km behind the front and a stable layer above (rapidly increasing potential temperature with height) which deepens with distance behind the front. The shallow stable layer from rain-cooled air ahead of the front is evident as well.

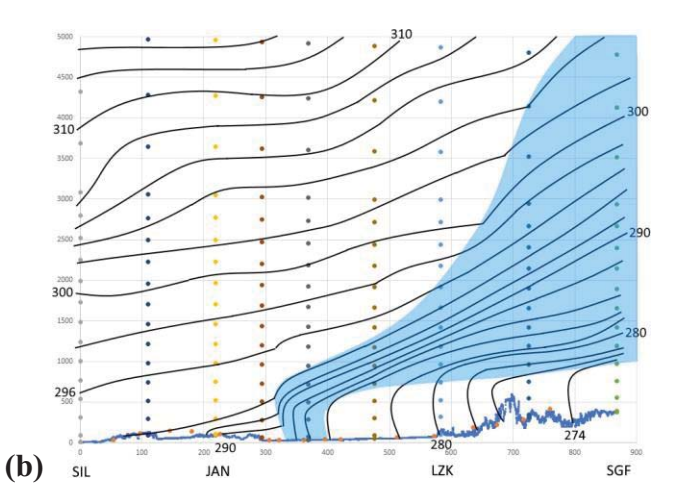


Figure 4: a) Skew-T log-p chart comparison of observed and NAM soundings behind cold front for approximately 1200 UTC at KLZK (Little Rock, Arkansas). **b)** Vertical cross-section of potential temperature (K) vs distance (km) at 1000 UTC between Slidell, Louisiana (SIL) and Springfield, Missouri (SGF), from synthesis of surface observations and NAM. Approximate extent of concentrated frontal zone shaded in blue.

MAY 2014 STATIONARY/COLD FRONT

A very different frontal system was observed on 17 May 2014. In broad terms, a cold front had reached central Mississippi on 16 May, moved back north as a warm front, stalled again, weakened, and then began to strengthen and move south again on the afternoon of the 17th. It was no longer connected to a well-organized low-pressure system and the air to the north of the boundary had moistened after widespread stratiform rain over the previous night (Fig. 5). In the upper troposphere, Mississippi was on the western (inactive) side of a deep trough in the polar jet stream (Fig. 6.a). Closer to the surface

(Fig. 6.b) a zonally oriented baroclinic zone stretched from Oklahoma to South Carolina with very little variation of geopotential height and a band of humid/cloudy conditions to the north. The 0000 UTC 18 May (corresponding to 7:00 PM Central Daylight Time on 17 May) surface conditions showed a well-defined wind shift across Mississippi, and temperatures dropping from 24 C to around 14 C in southwest Tennessee (Fig. 7). The afternoon MMU transect from near Holly Springs, Mississippi southward to Jackson (1946 UTC 17 May to 0059 UTC 18 May) did not encounter any rain, so that no consideration of wetbulbing was needed. The slowly moving front was intercepted at 2336 UTC, and data (including station data) are adjusted to this time.

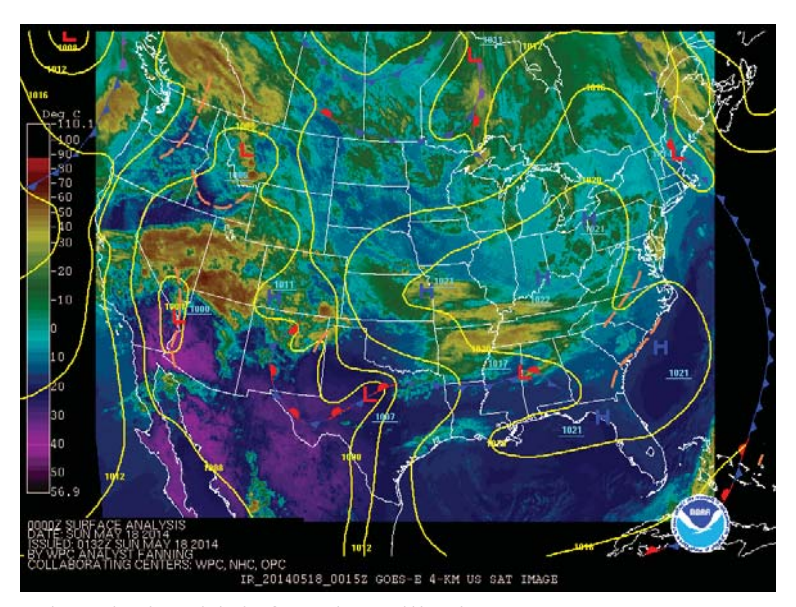


Figure 5: Surface frontal analysis with infrared satellite imagery at 0000 UTC on 18 May 2014.

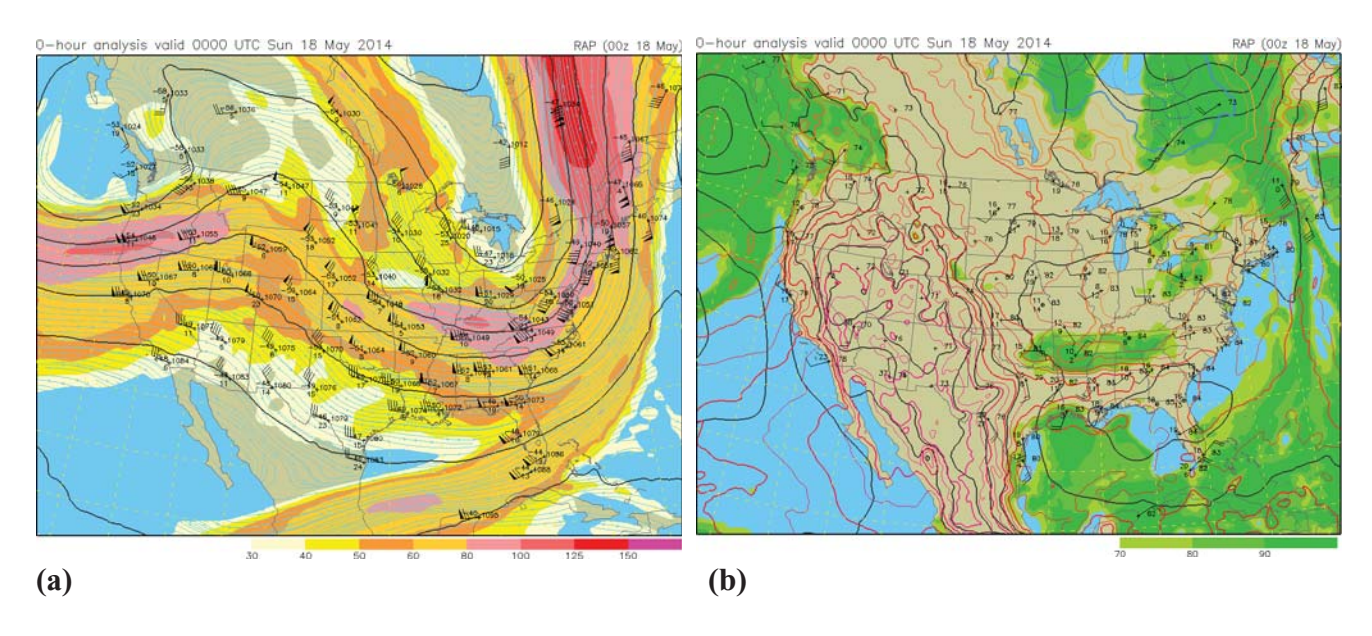


Figure 6: a) Radiosonde observations at 250 hPa from 0000 UTC 18 May 2014. Jet stream winds indicated by color shading in kt from hourly Rapid Update Cycle (RUC) model initial analysis. **b)** Radiosonde observations at 925 hPa from 0000 UTC 18 May 2014. Isotherms (red contours), geopotential height contours (black), and relative humidity (green shades above 70%) from RUC model initial analysis.

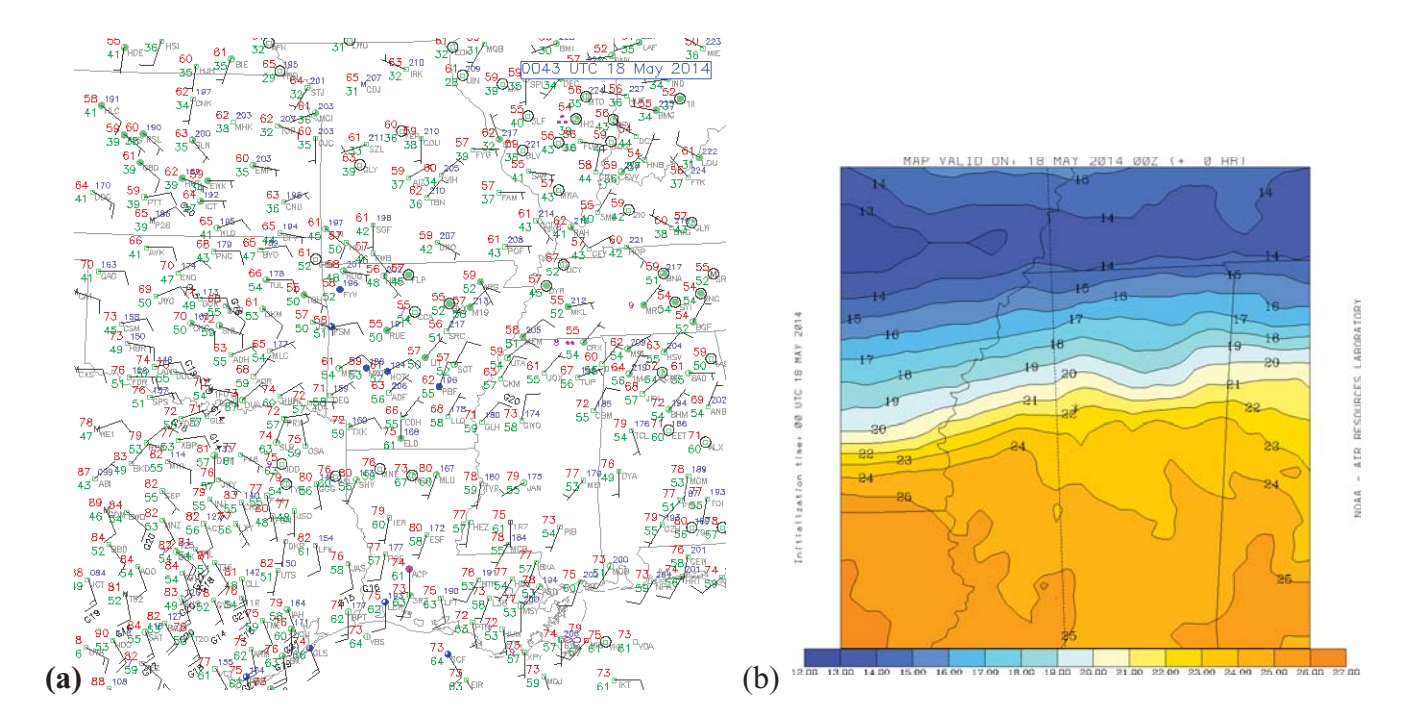


Figure 7: a) Surface synoptic observations at approximately 0000 UTC 18 May 2014: temperature/dewpoint in °F and winds in kt. **b)** Temperature pattern (°C) at surface over north Mississippi at 0000 UTC 18 May 2014 from NAM initial conditions. Note: Location of MMU frontal intercept is indicated by star.

Movement of the front during the day is shown by the 3-hourly NAM temperature analyses in Fig. 8. At 1500 UTC the southern temperature gradient was located around 33 N. By 2100 UTC it had moved north as a warm front to about 34 N. In the following three hours it again moved south as a cold front to about 33.5 N. It was therefore shortly after the transition back to southward movement that the MMU intercepted

the front. Subsequently the front continued to meander back and forth until finally dissipating on the 19th. A distinct confluent wind pattern (Fig. 9) is noted as a favorable frontogenetic influence to at least help maintain the frontal contrast in the absence of other supporting large-scale forcing.

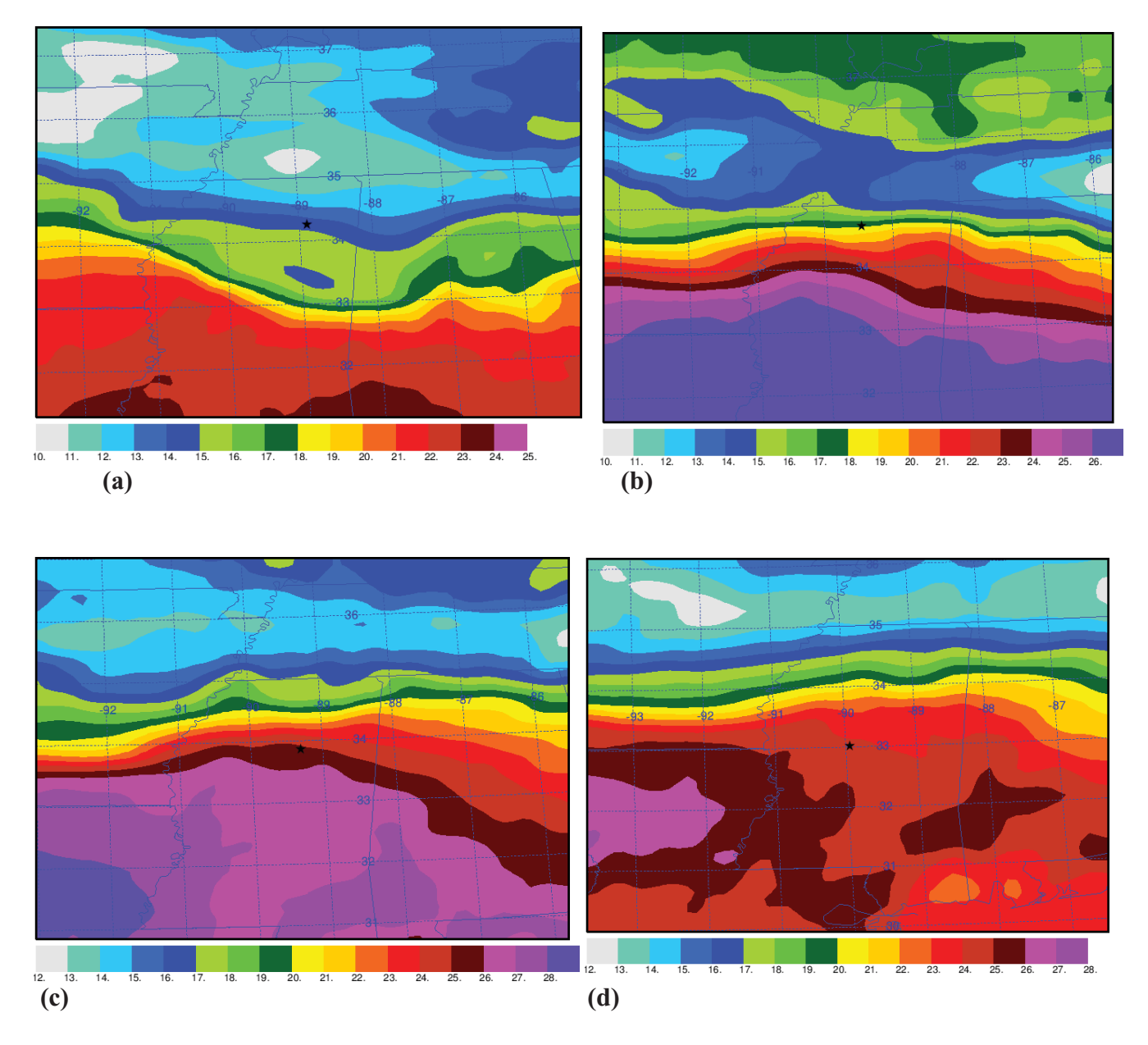


Figure 8: Temperature across Mississippi and surrounding states from NAM: **a)** 1500 UTC 17 May 2014; **b)** 1800 UTC 17 May 2014; **c)** 2100 UTC 17 May 2014; **d)** 0000 UTC 18 May 2014.

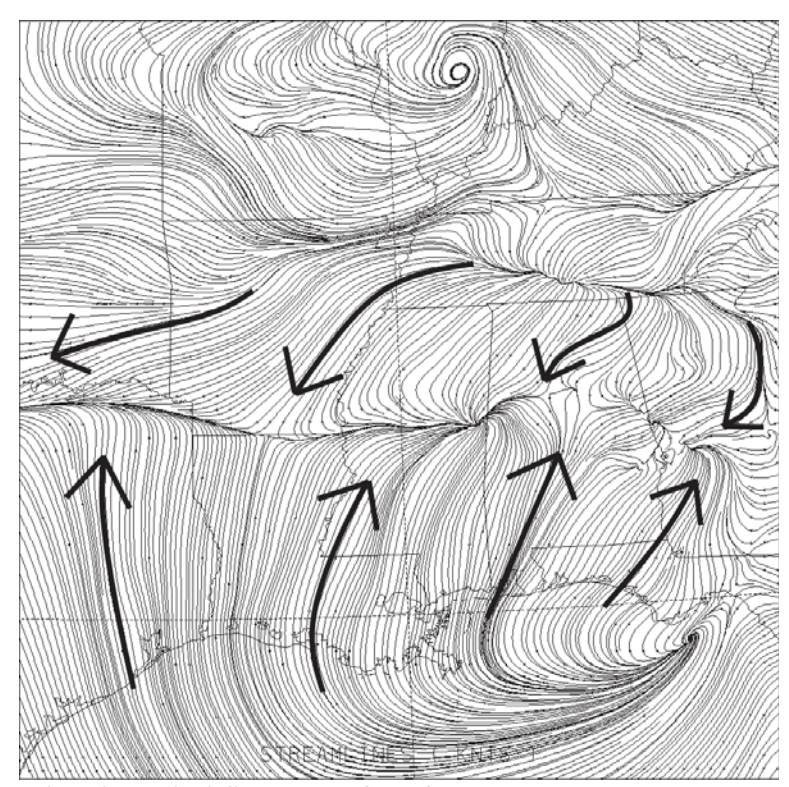


Figure 9: Streamlines showing wind flow at surface from NAM at 0000 UTC 18 May 2014.

A few notable features are seen in the mobile data. The variation of temperature and dewpoint relative to latitude is shown in Fig. 10.a, along with a comparison plot using only nearby observing stations. The detail of the mobile data more clearly shows the position of the front near

33.4 N, as well as the presence of a pre-frontal dry slot only about 15 km wide. Although one nearby observing station did indicate the anomalously low dewpoint, this one measurement would likely have been considered suspicious by an analyst in the absence of other corroborating data. Other than this dry slot, there was practically no difference between the prevailing dewpoint on each side of the front. While various researchers have looked at prefrontal troughs (Schultz 2005), wind shifts (Hutchinson and Bluestein 1998), and drylines, those typically are on a larger scale and tend to be associated with rapidly moving cold fronts instead of a quasi-stationary front. There is not enough information available to determine exactly what this particular feature is or how it formed.

However one interesting clue lies in the regional analysis of potential temperature (Fig. 10.b). While the wind flow shows a single well-defined line of confluence, there seem to be two separate transitions of potential temperature in eastern Mississippi that join into one in the west. This apparent split in the front is a short distance east of the MMU front intercept near Winona, leading speculation that perhaps somehow the anomalous dry slot is associated with processes related to development of the unusual split pattern in the front. There was no significant deep convection in the region that could have influenced the front at these scales. It may be that these anomalous patterns may relate to a form of discrete frontal propagation by a combination of diabatic and dynamical processes (Charney and Fritsch 1999; Bryan and Fritsch 2000). The visual change of cloud features observed north of the front, within the dry slot, and within the main warm air mass are exemplified in Fig. 11. Within only about 20 km, conditions went from broken low and mid-level stratus to only a few cirrostratus to poorly developed cumulus.

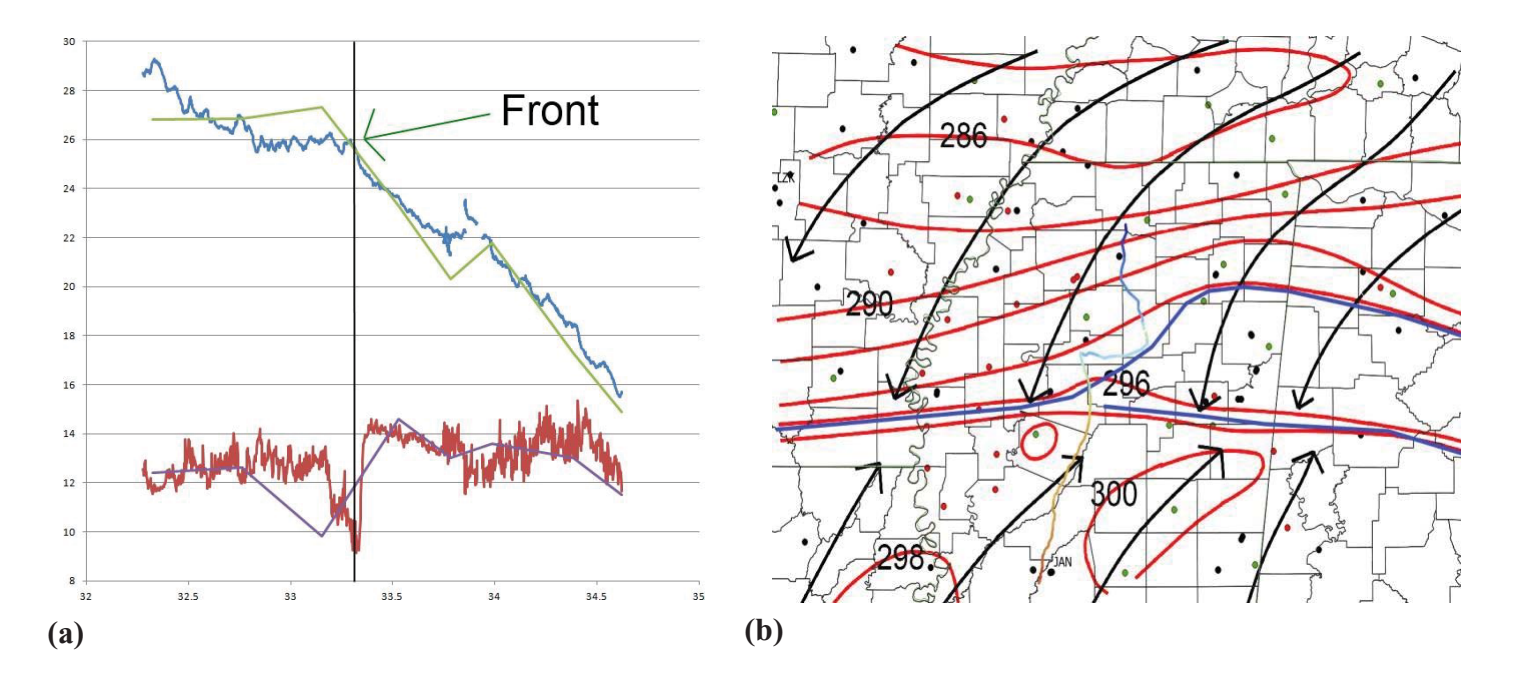


Figure 10: a) Temperature (blue) and dewpoint (red) vs latitude from mobile system, adjusted to 2336 UTC 17 May 2014. Temperature (green) and dewpoint (purple) from nearby stations. **b)** Manual analysis of wind flow and potential temperature (red) from synthesis of observing stations (dots) and mobile transect. Approximate front positions indicated by blue lines. Potential temperature from mobile platform indicated by color (red= maximum and blue = minimum).



Figure 11: a) Photograph from mobile platform north of front at 2315 UTC, looking to west in Grenada, MS. b) Looking to south at 2323 UTC into dry air pocket, from just north of the front. c) Looking to east at scattered clouds in warm moist air to south of front and dry air at 2347 UTC.

SUMMARY

The cases reported here represent two very different frontal scenarios for Mississippi. By incorporating data from a mobile platform crossing approximately orthogonal to the fronts together with various operational data from the surrounding region, similarities and differences in the structure are documented. Experience suggests that much more variety exists among other frontal cases in the region.

Key results from these cases that are in agreement with common conceptual models and previous studies include:

- Very close spatial consistency between the location of thermodynamic change (here understood to be the front) and the location of the confluent wind shift
- A very sudden change of pattern ("first-order discontinuity") of potential temperature at the front, with continuing decrease for hundreds of km further northward
- Presence of a thermal inversion or layer of increased static stability that connects with the surface frontal zone

Some features which seemed to be relatively unique to the specific cases examined include:

- A relatively loose relationship between frontal position and location of heavy precipitation when examined at small scales (< 50 km) (Case 1)
- A narrow pre-frontal dry slot in spite of no significant overall moisture contrast across the front, with possible relation to a frontal split or discrete jump (Case 2)

As the JSU MMU system has evolved in the period since 2012, several other types of frontal cases have been observed within Mississippi and other regions. The development of improved data sources and addition of new observing sites have also provided opportunities for continuing analysis to improve understanding and operational applications that address the variety of impacts and uncertainties related to the detailed features of frontal systems within the state.

ACKNOWLEDGEMENT

This work is based on data collection and analysis that has been funded by the NOAA Educational Partnership Program under Agreements NA11SEC4810003 and NA17AE1623, as part of the NOAA Center for Atmospheric Sciences (NCAS) and the NOAA Center for Atmospheric Science and Meteorology (NCAS-M). The

contents are solely the responsibility of the author and do not necessarily represent the official views of the U.S. Department of Commerce/NOAA. Additional funding was provided by the U.S. National Science Foundation (1644888). The author gratefully acknowledges the NOAA/Air Resources Laboratory (ARL) and Iowa Environmental Mesonet (Iowa State University) for data access.

CONFLICT OF INTEREST

There is no conflict of interest to declare.

LITERATURE CITED

Bjerknes, J., and H. Solberg, 1922: Life cycle of cyclones and polar front theory of atmospheric circulation. *Geof. Publ.*, **3**, 1–18.

Bluestein, H. B., Z. B. Wienhoff, D. D. Turner, D. W. Reif, J. C. Snyder, K. J. Thiem, and J. B. Houser, 2017: A comparison of the fine-scale structures of a prefrontal wind-shift line and a strong cold front in the Southern Plains of the United States. *Mon. Wea. Rev.*, **145**, 3307-3330.

Blumen, W., N. Gamage, R. L. Grossman, M. A. LeMone, and L. J. Miller, 1996: The low-level structure and evolution of a dry arctic front over the central United States. Part II: Comparison with theory. *Mon. Wea. Rev.*, **124**, 1676-1692.

Bryan, G. H., and J. M. Fritsch, 2000: Diabatically driven discrete propagation of surface fronts: A numerical analysis. *J. Atmos. Sci.*, **57**, 2061-2079.

Charney, J. J., and J. M. Fritsch, 1999: Discrete frontal propagation in a non-convective environment. *Mon. Wea. Rev.*, **127**, 2083-2101.

Demoz, B. B., D. O'C. Starr, K. D. Evans, A. R. Lare, D. N. Whiteman, G. Schwemmer, R. A. Ferrare, J. E. M. Goldsmith, and S. E. Bisson, 2005: The cold front of 15 April 1994 over the central United States. Part I: Observations. *Mon. Wea. Rev.*, **133**, 1525-1543.

Doswell III, C. A., and M. J. Haugland, 2007: A comparison of two cold fronts—Effects of the planetary boundary layer on the mesoscale. *E-Journal of Severe Storms Meteorol.*, **2**, no. 4.

Friedrich, K., D. E. Kingsmill, C. Flamant, H. V. Murphey, and R. M. Wakimoto, 2008: Kinematic and moisture characteristics of a nonprecipitating cold front observed during IHOP. Part I: Across-front structures. *Mon. Wea. Rev.*, **136**, 147-172.

Geerts, B., R. Damiani, and S. Haimov, 2006: Finescale vertical structure of a cold front as revealed by an airborne Doppler radar. *Mon. Wea. Rev.*, **134**, 251-271.

Hutchinson, T. A., and H. B. Bluestein, 1998: Prefrontal wind-shift lines in the plains of the United States. *Mon. Wea. Rev.*, **126**, 141-166.

Koch, S. E., and W. L. Clark, 1999: A nonclassical cold front observed during COPS-91: Frontal structure and the process of severe storm initiation. *J. Atmos. Sci.*, **56**, 2862-2890.

Mahre, A., T.-Y. Yu, R. Palmer, and J. Kurdzo, 2017: Observations of a cold front at high spatiotemporal resolution using an X-band phased array imaging radar. *Atmosphere*, **8**, 30.

Miller, L. J., M. A. LeMone, W. Blumen, R. L. Grossman, N. Gamage, and R. J. Zamora, 1996: The low-level structure and evolution of a dry arctic front over the central United States. Part I: Mesoscale observations. *Mon. Wea. Rev.*, **124**, 1648-1675.

Pietrycha, Albert E., and Erik N. Rasmussen, 2004: Finescale surface observations of the dryline: A mobile mesonet perspective. *Weather and forecasting*, **19**, 1075-1088.

Rolph, Glenn, Ariel Stein, and Barbara Stunder, 2017: Real-time environmental applications and display system: READY. *Environmental Modelling & Software*, **95**, 210-228.

Sanders, F., 1955: An investigation of the structure and dynamics of an intense surface frontal zone. *J. Meteorol.*, **12**, 542-552.

Schultz, D. M., 2005: A review of cold fronts with prefrontal troughs and wind shifts. *Mon. Wea. Rev.*, **133**, 2449-2472.

Shapiro, M. A., 1984: Meteorological tower measurements of a surface cold front. *Mon. Wea. Rev.*, **112**, 1634-1639.

Straka, J. M., E. N. Rasmussen, and S. E. Fredrickson, 1996: A mobile mesonet for finescale meteorological observations. *J. Atmos. Oceanic Tech.*, **13**, 921-936.

Wakimoto, R. M., and B. L. Bosart, 2000: Airborne radar observations of a cold front during FASTEX. *Mon. Wea. Rev.*, **128**, 2447-2470.

White, L., and J. Finney, 2005: A descriptive survey of meteorological observing systems in Mississippi. *J. of Miss. Acad. of Sci.*, **50**, 213-223.

White, L., 2014: Mobile observations of a quasi-frontal transient moisture boundary in the Deep South. *Weather and Forecasting*, **29**, 1356-1373, DOI: http://dx.doi.org/10.1175/WAF-D-14-00009.1